Physical limits to acceleration of enzymatic reactions inside phase-separated compartments

Jeremy D. Schmit [1,*] and Thomas C. T. Michaels [2,3,†]
[1]*Department of Physics, Kansas State University, Manhattan, Kansas 66506, United States*
[2]*Department of Biology, Institute of Biochemistry, ETH Zurich, Otto Stern Weg 3, 8093 Zurich, Switzerland*
[3]*Bringing Materials to Life Initiative, ETH Zurich, Switzerland*

(Received 8 November 2022; accepted 26 April 2024; published 3 June 2024)

We present a theoretical analysis of phase-separated compartments to facilitate enzymatic chemical reactions. While phase separation can facilitate reactions by increasing local concentration, it can also hinder the mobility of reactants. In particular, we find that the attractive interactions that concentrate reactants within the dense phase can inhibit reactions by lowering the mobility of the reactants. This mobility loss severely limits the potential to enhance reaction rates. Phase separation provides greater benefit in situations where multiple sequential reactions occur and/or high order reactions, provided the enzymes are unsaturated, transport to the condensate is not limiting, and the reactants are mobile. We show that mobility can be maintained if recruitment to the condensed phase is driven by multiple attractive moieties that can bind and release independently. However, the spacers necessary to ensure independence between stickers are prone to entangle with the dense phase scaffold. We find an optimal sticker affinity that balances the need for rapid binding/unbinding kinetics and minimal entanglement. Reaction rates can be accelerated by shrinking the size of the dense phase with a corresponding increase in the number of stickers. Our results showcase the potential capabilities of phase-separated compartments to act as biochemical reaction crucibles within living cells.

DOI: 10.1103/PhysRevE.109.064401

I. INTRODUCTION

In recent years many cellular structures, including nucleoli, Cajal bodies, stress granules, and P-bodies, have been found that form by the spontaneous condensation of biomolecules [1–4]. These structures, termed membraneless organelles (MLOs) or biomolecular condensates, form via liquid-liquid phase separation and typically contain tens to hundreds of different molecular components that are enriched in concentration relative to the surrounding environment [1–4]. Usually, only a small subset of these components, called "scaffolds," are necessary to drive condensation. The remaining components, classified as "clients," are not essential for condensation but are recruited by interactions with the scaffolds [2,4,5].

The biological function of MLOs remains a subject of intense research [3]. While experiments have revealed a variety of functions in well-studied systems [6–9], in most cases the function has not been established. Proposed functions include environmental sensing [7], stress response [8], signaling control [9], concentration buffering [10], and, in general, compartmentalization of biomolecular reactions in the cell [11]. In particular, it has been noted that MLOs could assist reaction kinetics by creating subcompartments with locally increased reactant concentrations [12–16]. However, the increased concentration also has the inhibitory effect of higher viscosity due to crowding effects [1,17,18] and reduced client mobility due to interactions with the scaffold. It therefore remains unclear to what extent MLOs can act as reaction crucibles to accelerate biochemical reactions.

Here, we use a simple theoretical model to explore the effectiveness of MLOs at accelerating enzymatic reactions between clients. We find that the attractive interactions that recruit substrate and enzyme molecules to a MLO can impair reaction dynamics by reducing diffusion. Phase-separated condensates contribute positively to chemical reactions when mobility is preserved within the condensed phase. This can be achieved by recruiting client molecules to the condensed phase through multiple independent attractive interactions, or "stickers," that allow for binding and release. However, the "spacers" required to maintain independence between these attractive interactions are susceptible to entangling with the scaffold of the dense phase. "Stickers" are regions in proteins or biomolecules that enable attractive interactions essential for phase separation. "Spacers," on the other hand, are interspersed regions that regulate the interactions between stickers, influencing the density, size, and dynamics of condensates without directly driving phase separation. We identify an optimal affinity for the attractive sticker interactions that strikes a balance between the need for rapid binding and unbinding kinetics and minimal entanglement. To accelerate reaction rates, we propose shrinking the size of the dense phase while increasing the number of attractive interactions, or "stickers" [19,20]. Thus it is most beneficial for large reaction orders where the strong concentration dependence can overwhelm the inhibitory effects of client binding. These results shed light on the physical limits on how much phase-separated compartments can affect biochemical reactions.

*schmit@phys.ksu.edu
†thomas.michaels@bc.biol.ethz.ch

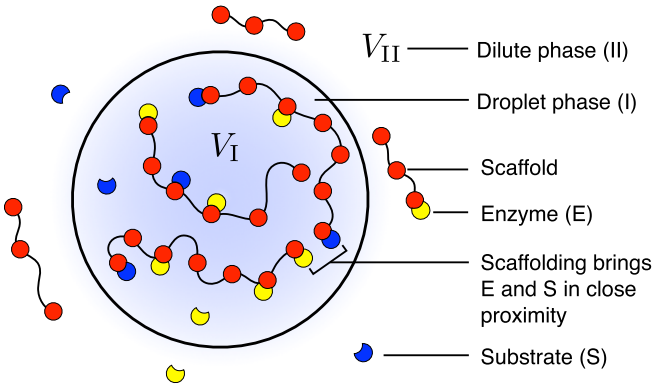

FIG. 1. Scaffolding of enzymatic reactions by biomolecular condensates. A system of total volume V_{tot} contains a condensate of volume V_I, which is formed by phase separation of a polymer scaffold. The condensate coexists with a dilute phase of volume V_{II}. Substrate S and enzyme E undergo an enzymatic reaction and are clients of the condensate. The scaffold-client interaction is described in terms of sites on the scaffold that substrate and enzyme molecules can bind to (scaffolding). Since the scaffold is highly concentrated in the condensate, substrate and enzyme are strongly recruited to the condensate. In addition, tethering of reactants to the scaffold can bring substrate and enzyme in close proximity facilitating the reaction [21].

II. MODEL CONSISTS OF A CONDENSATE SCAFFOLD NETWORK WITH BINDING SITES FOR ENZYMES AND SUBSTRATES

We consider a system of volume V_{tot} containing a biomolecular condensate of volume V_I (Fig. 1). The condensate forms through phase separation of a polymer scaffold with respect to the surrounding solution, resulting in a scaffold-rich droplet phase I stably coexisting with a dilute phase II of volume $V_{II} = V_{tot} - V_I$. Within this system, an enzymatic reaction takes place, involving the formation of product P from a substrate S and an enzyme E that are both clients of the condensate. This means that S and E molecules are not directly driving phase separation, but partition in phase I or phase II depending on their relative interactions with the condensate scaffold. We describe these interactions between the clients and the scaffold in terms of sites on the scaffold that clients can bind to (see Appendix A). With this model we can describe situations where the enzymes are covalently linked to the scaffolds with small rapidly diffusing substrates [14,15] or the clients are recruited by specific binding modules [22]. Moreover, in Sec. III E, we consider the situation when substrates are produced within the condensate. The ratios $p_S = S_I/S_{II}$ and $p_E = E_I/E_{II}$ are the partitioning degrees of S and E molecules and, for simplicity, in the following we assume that the enzyme and substrate are recruited to the condensate by equivalent interactions resulting in identical partition coefficients $p_S = p_E = p$. To characterize the rate of the enzymatic reaction in both phases, we employ the Michaelis-Menten-Hill equation

$$R_i = \frac{k_i E_i S_i^n}{K_{M,i}^n + S_i^n}, \tag{1}$$

where E_i, S_i are the local concentrations of enzyme and substrate in phase $i = \mathrm{I}, \mathrm{II}$. The phase-dependent reaction rate constants are denoted as k_i, while n is the Hill coefficient, describing the reaction order with respect to the substrate concentration. We introduce a scaffold-dependent Michaelis-Menten constant $K_{M,i}$ (referred to as scaffolded K_M hereafter, see Appendix B), to address the changes in molecular organization of clients caused by scaffolding [21]. The process of binding to the scaffold brings the substrate and enzyme in close proximity, resulting in a reduction of the Michaelis-Menten constant (K_M) compared to the homogeneous system, i.e., the enzymes saturate at a lower substrate concentration [21]. It is likely that scaffolding can lead to diverse organizations of bound enzymes and substrates, thereby resulting in a distribution of different K_M values; thus, $K_{M,i}$ is an average from this distribution [21].

III. RESULTS

A. Reaction rate enhancement by condensate is maximal at low substrate concentrations

To evaluate the potential of condensates in enhancing reactions, we quantitatively compared the average reaction rate in the phase-separated system to that in an equivalent homogeneous system. In the homogeneous system, the reaction rate R_{homo} can be expressed as

$$R_{homo} = \frac{k \bar{E} \bar{S}^n}{K_M^n + \bar{S}^n}, \tag{2}$$

where $\bar{S} = \phi S_I + (1-\phi) S_{II}$ represents the average substrate concentration, and $\bar{E} = \phi E_I + (1-\phi) E_{II}$ represents the average enzyme concentration. The parameter $\phi = \frac{V_I}{V_{tot}}$ denotes the volume fraction of the dense phase. In the phase-separated system, the volume-averaged reaction rate is given by $\bar{R} = \phi R_I + (1-\phi) R_{II}$. Using conservation of mass in combination with Eqs. (1) and (2), we calculated the reaction rate enhancement, defined as $\mathcal{E} = \bar{R}/R_{homo}$ (see Appendix E for details). Our analysis reveals that the rate enhancement $\mathcal{E}$ is dependent on six dimensionless parameters. These include the partitioning degree p and the volume fraction of the dense phase ϕ, as well as four additional dimensionless parameters: $\sigma = \frac{\bar{S}}{K_M}$, $\kappa = \frac{k_I}{k_{II}}$, $\mu = \frac{K_M}{K_{M,I}}$, and $\omega = \frac{K_{M,II}}{K_{M,I}}$. σ describes the average substrate concentration $\bar{S}$ normalized by the Michaelis-Menten constant K_M, μ is the ratio between the bulk Michaelis-Menten constant and the scaffolded K_M, and κ quantifies the difference between the rate constants in the dense phase k_I and dilute phase k_{II}. Figure 2(a) displays the dependence of the reaction rate enhancement on the condensate volume fraction, ϕ, and the normalized concentration of substrate, $\sigma = \frac{\bar{S}}{K_M}$, while keeping client partitioning constant. We see that the highest rate enhancement by the condensate occurs for low substrate concentration, $\sigma < 1$. However, as the substrate concentration increases, $\sigma > 1$, $\mathcal{E}$ decreases. Under these circumstances, the reaction rate remains unaffected by the presence of the condensate, and, if $\kappa < 1$, such recruitment can even lead to inhibition of the reaction. This insensitivity to concentration is because the enzymes saturate above $\sigma \simeq 1$. We further explored the dependence of the rate enhancement $\mathcal{E}$ on the partitioning coefficient and substrate concentration,

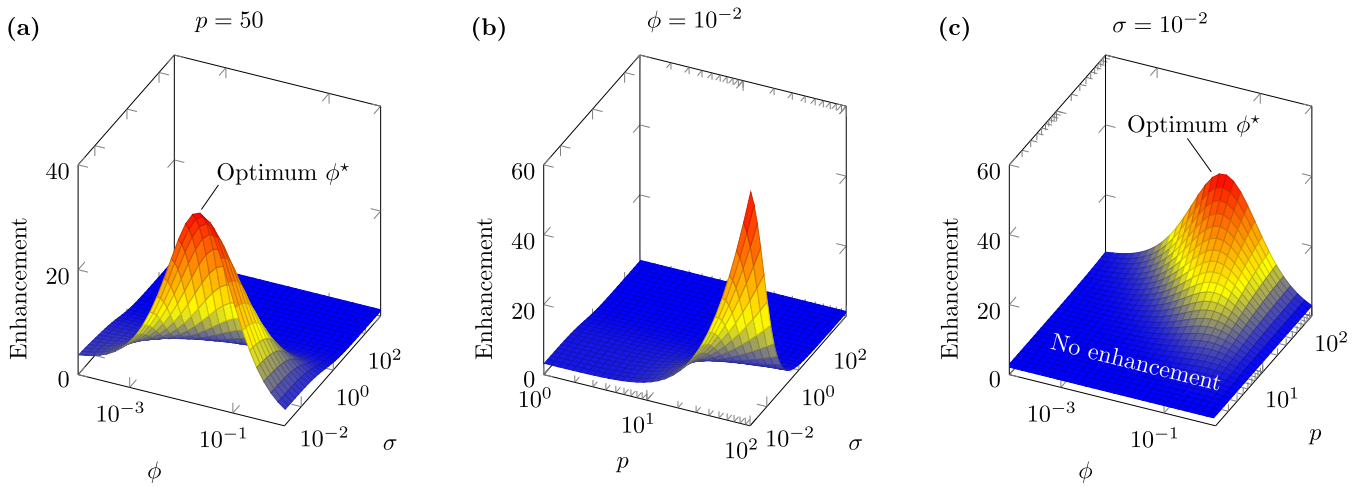

FIG. 2. Reaction rate enhancement $\bar{R}/R_{\text{hom}}$ as a function of condensate volume fraction ϕ and substrate concentration σ (a), partitioning degree p and substrate concentration σ (b), condensate volume fraction ϕ and partitioning degree p (c). The plots are shown at constant $p = 50$ (a), $\phi = 10^{-2}$ (b), or $\sigma = 10^{-2}$ (c), respectively. The remaining parameters are $\mu = 3$, $\omega = 1$, $\kappa = 1$, $n = 1$, equal for all three panels.

while keeping the droplet volume constant [Fig. 2(b)]. When the substrate concentration is low, $\sigma < 1$, increasing the partition coefficient p results in a higher overall rate enhancement. This occurs because the reacting clients are concentrated and colocalized in the condensed phase. However, as we increase the substrate concentration, $\sigma > 1$, client partitioning into the condensate ceases to have an effect on the total reaction rate, as seen above because the enzymes saturate and the reaction becomes concentration independent.

B. Small condensates optimize overall reaction rate

Figure 2 indicates that substrates with a total concentration that is significantly lower than the Michaelis-Menten constant (K_M) can experience enhancement when they are recruited, along with enzymes, into condensates. On the other hand, substrates with concentrations that are higher relative to K_M do not benefit from condensation. In fact, in some cases, such recruitment can even lead to inhibition of the reaction. The strongest reaction rate enhancement by the condensate occurs in the limit when substrate concentration is low, $\sigma \to 0$, and the local rate is approximately $R_i = (k_i/K_{M,i}^n)E_i S_i^n$. In this limit, the rate enhancement $\mathcal{E}$ can be written as (see Appendix E):

$$\mathcal{E} = \frac{\bar{R}}{R_{\text{homo}}} = \left(\frac{\mu}{\omega}\right)^n \frac{1 - \phi + \phi\omega^n\kappa\, p^{n+1}}{(1 - \phi + \phi\, p)^{n+1}}. \tag{3}$$

Interestingly, we find that the rate enhancement $\mathcal{E}$ displays a maximum with ϕ [Figs. 2(a) and 2(c)]. The optimal condensate volume fraction $\phi^\star$ can be obtained by maximising $\mathcal{E}$ with respect to ϕ holding p constant, which yields

$$\phi^\star = \frac{(\omega^n\kappa\, p^{n+1} - 1) - (n+1)(p-1)}{n(p-1)(\omega^n\kappa\, p^{n+1} - 1)}. \tag{4}$$

The optimum $\phi^\star$ emerges from two opposing effects: on the one side, the contribution of R_{I} to the average reaction rate $\bar{R}$ decreases with decreasing ϕ; on the other side, lowering the condensate volume fraction ϕ causes the reaction rate in the droplet phase, R_{I}, to increase because smaller condensates achieve a higher local concentration. A small condensate volume ensures that the dilute phase is minimally depleted, which for fixed p maximizes concentrations in the dense phase. As shown in Appendix D, small condensates also help reduce diffusive transport as a limiting factor. The optimal volume fraction $\phi^\star$ decreases with increasing p and is inversely proportional to the reaction order n in the limit of large p and n. This is because large reaction orders are so sensitive to concentration that it is more beneficial to have a small reaction volume that is highly saturated than to have a larger reaction volume at lower concentration.

C. The optimal sticker affinity is a tradeoff between binding kinetics and entanglement

A necessary requirement for a reaction to occur is S and/or E must have enough mobility for intermolecular collisions. This mobility will be inhibited by the attractive interactions that recruit molecules to a condensate. In Appendix D, we show that the enhanced concentration from condensation is not beneficial if recruitment immobilizes one of the species. While bound molecules may retain a limited ability to explore a local volume due to network dynamics or flexible tethers, it is still necessary for the incoming substrates to diffuse within the condensate. This brings the question of how to achieve the optimal balance of recruitment and mobility.

Condensate scaffolds are not uniformly attractive and, instead, have discrete sticky moieties responsible for condensation and client recruitment [19,20]. Bound clients can remain mobile if they have the same sticker-and-spacer architecture as the scaffolds because independent stickers allow some parts of the molecule to move while other parts remain bound. While the sticker/spacer structure allows the client to move without detaching from the condensate scaffold, it comes at a price because the spacers that allow stickers to bind/unbind independently are prone to entangle with the scaffold. As a result, the client molecules transition from Stokes diffusion outside the condensate to reptation inside [23,24]. Thus, if a certain level of recruitment is required,

there is a tradeoff between a small number of stickers that bind tightly or a large number of weak stickers that are highly entangled. The optimum between these extremes can be found from the dependence of the affinity and mobility on the number of stickers.

The most favorable case for facilitating reactions is when there are abundant binding sites for clients, in which case the free energy change for a client molecule with M stickers entering the condensate is (see Appendix A)

$$\Delta F/k_BT = -\ln(p) = -M\ln(1+e^{-\epsilon}), \tag{5}$$

where $\epsilon = \Delta f/k_BT$ is the free energy difference between the bound and unbound states of a sticker and p is the partitioning degree. We note that the linear scaling of Eq. (5) with M agrees with previous experiments [6]. The diffusion constant for a polymer undergoing reptation will be proportional to $D_{\text{client}} \propto r_g^2/\tau_{\text{rep}}$ indicating that the polymer has moved a distance proportional to its radius of gyration r_g during a reptation time τ_{rep}. The reptation time scales as $\tau_{\text{rep}} \propto \ell^2/D_\parallel$, where $D_\parallel$ describes diffusion in the direction parallel to the polymer length ℓ. This diffusion depends on the length of the polymer $D_\parallel \propto 1/\ell$, where the unknown constant describes the diffusion of a chain subunit. In this context the repeating unit has contributions from spacer and the adjoining sticker. We assume that, for the sticker-spacer unit to move through the network, the sticker must be in the unbound state. Therefore we have

$$D_\parallel \propto \frac{D_{\text{spacer}}}{M(1+e^{-\epsilon})}, \tag{6}$$

where we have used $\ell \propto M$. Thus we find

$$\tau_{\text{rep}} \propto \frac{M^3(1+e^{-\epsilon})}{D_{\text{spacer}}}. \tag{7}$$

After a time τ_{rep}, the polymer will move by a distance $r_g \propto \sqrt{M}$. Therefore the diffusion constant of client molecules is

$$D_{\text{client}} \propto \frac{D_{\text{spacer}}}{M^2(1+e^{-\epsilon})}. \tag{8}$$

In Eq. (8), the diffusion coefficient scales with polymer size M as $D_{\text{client}} \propto M^{-\gamma}$ with $\gamma = 2$, which corresponds to polymers that are entangled by neighboring polymers and can escape via reptation. It is important to note that such scaling exponents apply to homogeneous systems consisting of a single phase. However, biological systems, such as the cytoplasm, are often heterogeneous and composed of various components and condensed phases [25–28]. To address this complexity of biological environments, we could consider varying rheology exponents $D_{\text{client}} \propto M^{-\gamma}$ with $0.5 \leqslant \gamma \leqslant 2$ to accommodate scenarios involving polymer melts or microphase-separated mixtures. In the case $\gamma = 2$ and using Eq. (5), we optimize D_{client} with respect to M holding the partitioning, p, or equivalently, the total affinity, $A = \Delta F/k_BT$, fixed. This yields $A/M = -2$ and therefore an optimal binding free energy for a sticker $\Delta f \simeq -1.85\,k_BT$, which includes the sticker-sticker interaction and the conformational entropy loss of the spacer (see Appendix E for details). This value allows the sticker to bind and release frequently enough for the molecule to diffuse, but provides enough affinity the molecule does not become too long and entangled. Therefore the partition coefficient of a dynamically optimized client is $p = e^{2M}$.

An important case that is not explicitly covered by our calculations is that of electrostatic coacervates. We expect that these will behave similarly to our reptation calculation, although the smooth charge distribution on molecules like RNA violates our approximation of independent stickers. Another complication is that the neutralization afforded by complementary charged scaffolds will perturb the conformational ensembles and stabilize compact and/or double stranded states [12,13,16].

D. Reaction rates are enhanced for high order reactions

Using the optimal sticker affinity, we can determine the level of client recruitment to maximize the reaction rate. We assume that the dense phase reaction rate is proportional to the client diffusion constant so $\omega^n\kappa = \alpha/M^2$, where α is a constant accounting for the transition between Stokes and reptation dynamics (see Appendix E for details). Figure 3(b) shows $\mathcal{O}(10^3)$ enhancement for $n = 2$. Greater enhancements are found for larger reaction orders (see Fig. 7), which shows why condensates are prone to the nucleation of aggregates [29] and why they are useful for the assembly of large complexes like viral capsids [30,31]. Conversely, for small reaction orders it is difficult to get any rate enhancement. Figure 8 shows that $n = 1$ reactions require $\phi < 10^{-3}$ and $M \sim 5$, which corresponds to recruitment affinities $>10k_BT$, to achieve even modest enhancements (less than tenfold). This regime may not be physically realistic because the high concentration of clients will compete for available stickers, voiding the independent molecule approximation of Eq. (5), and limiting the achievable values of p.

E. Condensates make multistep reactions more efficient

Although condensates can facilitate reactions by concentrating reactants, the attractive interactions responsible for localization have an inhibitory effect on reaction kinetics. However, it is possible to achieve enhanced concentrations without a loss in mobility if the reactants are produced within the condensate itself. Localized production will provide a concentration gradient that will benefit subsequent reactions provided the reactions occur faster than the reactants diffuse away. Here we show that localizing sequential reactions within a condensate will make the later steps more efficient in the sense that there will be lower levels of unreacted intermediate. However, the overall reaction rate is fixed by the substrate production rate and, therefore, is not enhanced by the condensate.

When substrate is produced within the condensate there is the possibility for locally enhanced substrate concentration if diffusive transport of substrate is sufficiently slow. An example of such a situation is the production of ribosomes within the nucleolus requires multiple steps including RNA transcription, splicing, folding, and assembly with ribosomal proteins [32]. Sequential reactions can be handled by introducing a source term Σ. This addition results in two kinetic regimes. At short times, $t\,\Sigma < (\phi S_{\text{I}}(0) + (1-\phi)S_{\text{II}}(0))$, the substrate generated by the source is negligible compared to

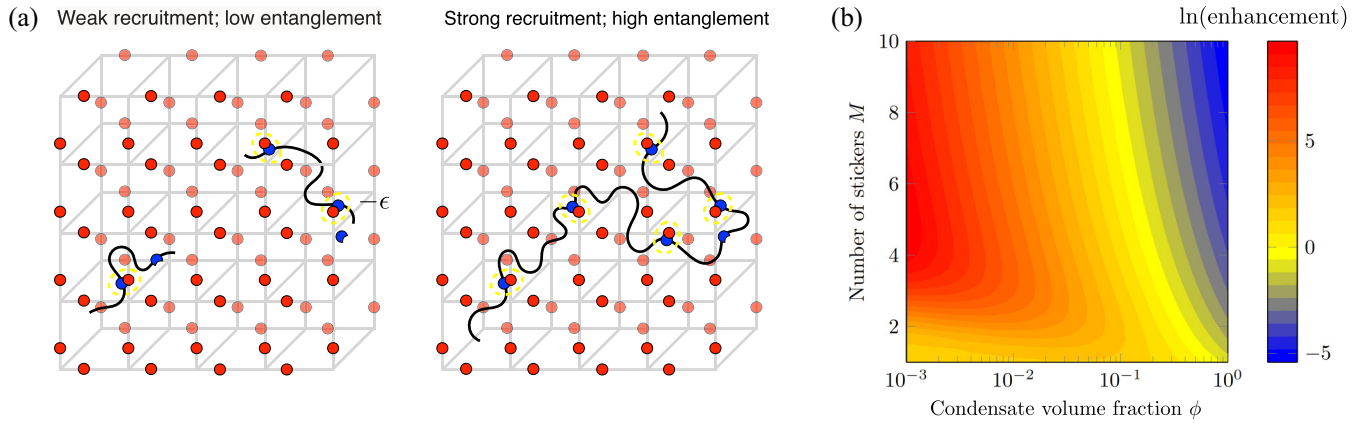

FIG. 3. Optimal sticker affinity to balance client partitioning and entanglement. (a) Increasing the number of stickers increases client recruitment, but the clients become highly entangled with the scaffold, slowing diffusion. Optimal mobility, for fixed affinity, occurs when the stickers have a binding free energy of $\Delta f \sim 2\,k_BT$. (b) Ratio of the reaction rate for a separated system to a homogeneous system ($\mathcal{E} = \bar{R}/R_{\rm hom}$) as a function of the condensate volume fraction ϕ and the number M of stickers with binding energy $\Delta f \sim 2\,k_BT$. When ϕ is sufficiently small there is an optimal number of stickers M, and hence p (since $p = e^{2M}$), that maximizes the reaction rate. $M = 4$ corresponds to $p \simeq 3000$. The parameters are: $n = 2$, $\alpha = 0.1$.

the substrate present at $t = 0$ (Fig. 4). However, at long times, substrate production dominates and the system approaches a steady state in which the condensate plays a beneficial role. Since localization is achieved by substrate production, we can understand the enhancement by neglecting the binding terms

$$\frac{dS_{\rm I}}{dt} = k_{\rm diff}(S_{\rm II} - S_{\rm I}) - kS_{\rm I}E_{\rm I} + \Sigma, \tag{9a}$$

$$\frac{dS_{\rm II}}{dt} = -\frac{\phi}{1-\phi}k_{\rm diff}(S_{\rm II} - S_{\rm I}) - kS_{\rm II}E_{\rm II}. \tag{9b}$$

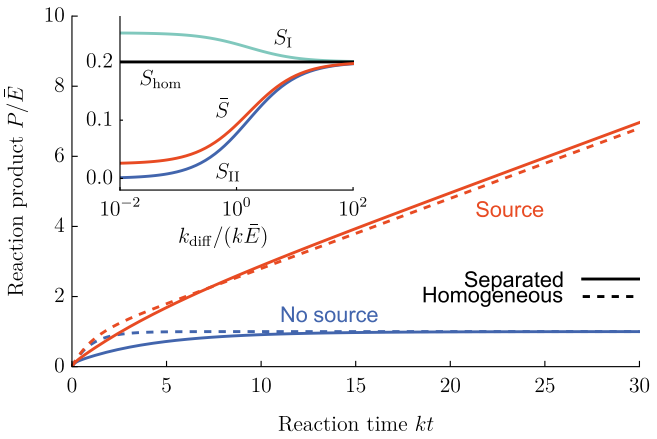

FIG. 4. When the supply of substrate is fixed (blue lines) recruitment of enzymes to a condensate inhibits product formation because the diffusive transport of substrate is limiting. When substrate is produced within the condensate (red lines) the system initially behaves like the fixed substrate system where the condensate is detrimental before converging to a steady state where the condensate is somewhat beneficial. (Inset) The steady-state concentrations of substrate in the dilute phase ($S_{\rm I}$), dense phase ($S_{\rm II}$), and total system ($\bar{S}$) all converge to that of the homogeneous system ($S_{\rm hom}$) when diffusion is very fast. $E_{\rm I}/E_{\rm II} = 8$, $k_{\rm diff}/(k\bar{E}) = 0.1$, $\phi = 0.1$, $\Sigma/(k\bar{E}) = 2$, and $S_{\rm I}(0) = S_{\rm II}(0) = \bar{E}$.

where we are considering the limit where the linearized rate constants in the dense and dilute phases are identical $k'_{\rm I} = k'_{\rm II} = k$. The steady-state solution to these equations is

$$\frac{S_{\rm I}}{S_\infty} = \frac{1 + (1-\phi)\frac{kE_{\rm II}}{k_{\rm diff}\phi}}{1 + (1-\phi)\frac{kE_{\rm II}E_{\rm I}}{k_{\rm diff}\bar{E}}}, \tag{10a}$$

$$\frac{S_{\rm II}}{S_\infty} = \frac{1}{1 + (1-\phi)\frac{kE_{\rm II}E_{\rm I}}{k_{\rm diff}\bar{E}}}, \tag{10b}$$

where $S_\infty = \bar{\Sigma}/(k\bar{E})$ is the homogeneous solution limit (equivalent to $k_{\rm diff} \to \infty$) and $\bar{\Sigma} = \phi\,\Sigma$. From this, we can see that the outside concentration $S_{\rm II}$ is always less than the homogeneous case (i.e., $S_{\rm II} < S_\infty$), while inside concentration $S_{\rm I}$ is always greater (i.e., $S_{\rm I} > S_\infty$), see inset of Fig. 4. To see the benefit of the condensate, we look at the average concentration of S

$$\bar{S} = (1-\phi)S_{\rm II} + \phi\,S_{\rm I} = S_\infty \frac{1 + (1-\phi)\frac{kE_{\rm II}}{k_{\rm diff}}}{1 + (1-\phi)\frac{kE_{\rm II}E_{\rm I}}{k_{\rm diff}\bar{E}}}, \tag{11}$$

which shows that $\bar{S}$ is always less than the homogeneous limit S_∞, since $E_{\rm I} > \bar{E}$ (Fig. 4, inset). Importantly, the condensate does not affect the overall reaction rate, which is fixed by the steady-state condition. However, the condensate ensures that there is less unused substrate. This is particularly useful for limiting the quantity of intermediate states in high-volume reactions like ribosome synthesis as well as situations where intermediate states are prone to pathogenic aggregation. The key features of Fig. 4 are (1) there is a crossover time before which the condensate is detrimental and after which the condensate is beneficial. After the crossover time, (2) the volume averaged substrate concentration and concentration of substrate outside the condensate are less than S_∞, (3) the concentration of substrate inside the condensate is greater than S_∞, and (4) all three of these values approach S_∞ as $k_{\rm diff} \to \infty$. These features are all robust to the parameter values.

IV. CONCLUSION

We have shown that the interactions that recruit reactants to phase separated compartments necessarily impair mobility, and hence reactivity. This mobility loss may be acceptable in situations with multiple sequential reactions or high order reactions, but in most cases reactions progress more rapidly when reactants are dispersed in the homogeneous state.

ACKNOWLEDGMENTS

We acknowledge support from Institute for the National Institutes of Health Grant No. R01GM141235.

APPENDIX A: RECRUITMENT EQUILIBRIUM AND CLIENT PARTITIONING

In this section, we compute how the microscopic characteristics of the network, such as the concentration of binding sites and their affinity, affect client recruitment. In particular, we are interested in the partition coefficient, defined as

$$p = \frac{S_{\mathrm{I}}}{S_{\mathrm{II}}}, \tag{A1}$$

which relates the client concentrations inside and outside of the condensate.

1. Single site binding

We first consider the situation where a client can only interact with one scaffold binding site at a time. The client concentration inside the condensate is the sum of soluble and bound species. We denote the soluble fraction S_{Is} and the bound fraction S_{Ib} such that $S_{\mathrm{I}} = S_{\mathrm{Is}} + S_{\mathrm{Ib}}$. We can relate the concentrations of soluble and bound species by the dissociation constant

$$K_D = \frac{(B - S_{\mathrm{Ib}})S_{\mathrm{II}}}{S_{\mathrm{Ib}}}, \tag{A2}$$

where B is the concentration of binding sites in the dense phase. If the system is in diffusive equilibrium the concentration of soluble species is equal inside and outside of the condensate. If the binding to free scaffold in the dilute phase is negligible then $S_{\mathrm{Is}} = S_{\mathrm{II}}$. The probability that a given site is occupied is given by

$$P_{\mathrm{bound}} = \frac{S_{\mathrm{Ib}}}{S_{\mathrm{Ib}} + (B - S_{\mathrm{Ib}})} = \frac{1}{1 + K_D/S_{\mathrm{II}}}. \tag{A3}$$

Therefore the total concentration of client inside the condensate is

$$S_{\mathrm{I}} = S_{\mathrm{II}} + \frac{B}{1 + K_D/S_{\mathrm{II}}}. \tag{A4}$$

The partition coefficient is then

$$p = 1 + \frac{B}{S_{\mathrm{II}} + K_D}. \tag{A5}$$

The usefulness of the partition coefficient is that it provides a measure of recruitment that does not depend on the concentration of client. From Eq. (A5), we can see that the concentration independence is only valid when $S_{\mathrm{II}} < K_D$. Below this threshold $p \simeq 1 + B/K_D$ and the concentration of client in the condensate rises linearly with the total concentration. However, when S_{II} approaches or exceeds K_D the binding sites begin to saturate and the partition coefficient declines because the soluble concentration rises faster than the bound fraction.

2. Sticker-and-spacer binding

a. Binding equilibrium

Next we calculate the concentration of polymer-like clients within a scaffold network. The extent of recruitment is determined by the condition that the chemical potential of the clients must be the same in the dilute and concentrated phases. The partition function for N clients is given by $Q_N = Q_1^N/N!$. This expression is valid in the dilute phase, but not necessarily in the dense phase. If recruitment to the dense phase is strong enough, it is necessary to account for interactions between the clients. These interactions will result in a competition for scaffold binding sites. As shown in the calculation for single site binding, this competition leads to a decline in the partition coefficient [Eq. (A5)] at large concentration. Therefore the calculation below represents an upper limit on the ability of a condensate to recruit clients and, hence, facilitate reactions. Our focus on optimized systems is to highlight the limited capacity of condensates to facilitate reaction kinetics.

The chemical potential of the clients is

$$\begin{aligned}\mu &= -k_B T \frac{\partial \ln(Q_N)}{\partial N} \\ &= -k_B T(\ln(Q_1) - \ln N),\end{aligned} \tag{A6}$$

where we used Stirling's approximation $\ln(N!) = N\ln(N) - N$ for $N \gg 1$. The next step is to evaluate Q_1 which we write as a product of position and conformation states $Q_1 = Q_{\mathrm{pos}}Q_{\mathrm{conf}}$. To evaluate the position partition function we choose one end of the polymer as a reference point and sum over all possible positions for this point of the polymer. Neglecting boundary effects, this integration yields the volume of the relevant phase divided by a microscopic parameter V_1 that sets the volume per state (similar to the Debye wavelength)

$$Q_{\mathrm{pos}} = V/V_1. \tag{A7}$$

Inserting this into the expression for chemical potential, Eq. (A6), we have

$$\mu = -k_B T(\ln(Q_{\mathrm{conf}}) - \ln(cV_1)), \tag{A8}$$

where $c = N/V$ is the client concentration.

To evaluate Q_{conf} we assume that the client molecule consists of M stickers and $M + 1$ spacers (i.e., both ends of the molecule terminate with a spacer). We further assume that each spacer is long enough, and that the number of scaffold binding sites is large enough, that each spacer is statistically independent. Each spacer has a fixed starting point that is determined by either the state in the position integration (for the first spacer) or the end point of the previous spacer (for the next M spacers). The partition function for each spacer consists of a sum over all possible end points given the fixed starting point. In the dilute phase, where we can neglect binding, each spacer is identical so

$$Q_{\mathrm{conf}} = Q_{\mathrm{spacer}}^{M+1}. \tag{A9}$$

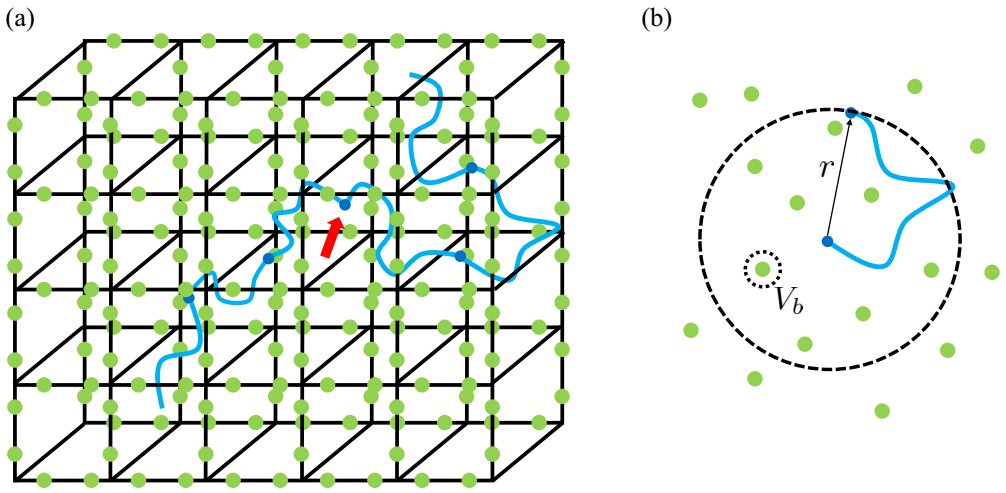

FIG. 5. Schematic of the geometry in the calculation of the client free energy. (a) The calculation describes a polymerlike client (blue) entangled with a scaffold matrix (black lines). Stickers on the client (dark blue dots) can interact with attractive patches (green dots) on the scaffold. The spacers are long enough, and the binding patches abundant enough, that the binding states of adjacent stickers are approximately independent. The figure shows a client with $M = 5$ stickers. Four of these stickers are bound to the scaffold but the middle one is unbound (red arrow). This independence allows the client to gradually move through the network. (b) The partition function for each spacer involves an integration over the end to end vector r. This integration will include states where the sticker at the end is unbound (as shown) and states with it bound to the scaffold binding sites (green dots). Each binding site is surrounded by a volume V_b within which the sticker is considered bound.

Q_{spacer} accounts for the Gaussian distribution of polymer states for fixed starting and ending points

$$Q_{\text{spacer}} = \frac{1}{V_1}\int e^{-r^2/r_g^2} d^3r, \tag{A10}$$

where r and r_g are the end-to-end vector and the radius of gyration of the spacer, respectively.

In the dense phase, we need to account for the fact that the first M spacers will have their conformational statistics perturbed by binding to the scaffold. However, the $(M+1)$th spacer, which does not contain a sticker is unperturbed by the scaffold (we neglect crowding effects). Therefore, in the dense phase, we have

$$Q_{\text{conf}} = Q_{\text{dense}}^M Q_{\text{spacer}}. \tag{A11}$$

The sum over states for the M spacers with stickers is similar to the dilute phase in that the starting point is fixed by either the position integration or the previous spacer. We account for the effect of the scaffold by splitting the integration into terms that result in either a free end or sticker-scaffold binding

$$\begin{aligned} Q_{\text{dense}} &= \frac{1}{V_1}\int e^{-r^2/r_g^2} d^3r + \sum_i^{\text{binding sites}} e^{-R_i^2/r_g^2}\left(e^{-\epsilon_b/k_BT} - \frac{V_b}{V_1}\right) \\ &= e^{-f_{\text{unbound}}} + e^{-f_{\text{bound}}}. \end{aligned} \tag{A12}$$

In the second term ϵ_b is the affinity of the sticker-scaffold binding interaction and R_i is the distance between the ith scaffold binding site and the beginning of the spacer. In writing the unbound integral, we have overcounted the volume accessible to the end of the spacer because each binding site on the scaffold will be surrounded by a volume V_b that results in a bound state. This overcounting is corrected by the V_b/V_1 term of the sum over binding states, which assumes that the V_b is small enough that R_i does not change appreciably within this volume (Fig. 5).

At equilibrium we have $\mu_{\text{dilute}} = \mu_{\text{dense}}$, which gives

$$\begin{aligned} &\ln\left(Q_{\text{spacer}}^{M+1}\right) - \ln\left(c_{\text{dilute}} V_1\right) \\ &\quad = \ln\left(Q_{\text{dense}}^M Q_{\text{spacer}}\right) - \ln\left(c_{\text{dense}} V_1\right). \end{aligned} \tag{A13}$$

This expression can be rearranged as follows:

$$\ln\left(\frac{c_{\text{dense}}}{c_{\text{dilute}}}\right) = \ln\left(\frac{Q_{\text{dense}}^M Q_{\text{spacer}}}{Q_{\text{spacer}}^{M+1}}\right) \tag{A14}$$

or

$$\begin{aligned} \frac{c_{\text{dense}}}{c_{\text{dilute}}} &= \left(\frac{Q_{\text{dense}}}{Q_{\text{spacer}}}\right)^M = \left(\frac{e^{-f_{\text{unbound}}/k_BT} + e^{-f_{\text{bound}}/k_BT}}{e^{-f_{\text{unbound}}/k_BT}}\right)^M \\ &= (1 + e^{-\Delta f/k_BT})^M, \end{aligned} \tag{A15}$$

where $\Delta f = f_{\text{bound}} - f_{\text{unbound}}$.

Our next task is to connect these free energies to the enrichment/depletion due to condensate formation. As defined in the text, the partition coefficient is given by

$$p = \frac{c_{\text{dense}}}{c_{\text{dilute}}} = (1 + e^{-\Delta f/k_BT})^M, \tag{A16}$$

Note that the binomial on the right hand side includes the unbound state so it is not necessary to include a S_{II} term as in Eqs. (A4) and (A5). Equation (A16) translates into a free energy change for a client molecule with M stickers entering the condensate

$$\Delta F/k_BT = -\ln(p) = -M\ln(1 + e^{-\Delta f/k_BT}), \tag{A17}$$

which is Eq. (5).

b. Sticker and spacer diffusion

Our next task is the optimize the mobility of the bound clients. To do this we start with the diffusion constant of the clients [Eq. (8)]

$$D_{\text{client}} \propto \frac{D_{\text{spacer}}}{M^2(1+e^{-\Delta f/k_BT})} \tag{A18}$$

and maximize with respect to M by keeping affinity $\Delta F/k_BT = A$ (or, equivalently, the partitioning p) constant. Using (A17), we write

$$1 + e^{-\Delta f/k_BT} = e^{-A/M}, \tag{A19}$$

which gives

$$D_{\text{client}} \propto \frac{e^{A/M}}{M^2} \quad \Rightarrow \quad \frac{\partial D_{\text{client}}}{\partial M} = -\frac{e^{A/M}}{M^3}\left(2+\frac{A}{M}\right) = 0 \quad \Rightarrow \quad \frac{A}{M} = -2. \tag{A20}$$

Therefore

$$1 + e^{-\Delta f/k_BT} = e^2 \quad \Rightarrow$$

$$\Delta f = -\ln(e^2-1)\,k_BT \simeq -1.85\,k_BT, \tag{A21}$$

which is about $2\ k_BT$. The partitioning of dynamically optimized clients is then

$$p = (1+e^{-\Delta f/k_BT})^M = e^{2M}. \tag{A22}$$

APPENDIX B: MICHAELIS-MENTEN ANALYSIS

1. Solution Michaelis-Menten

The basic Michaelis-Menten reaction scheme is

$$n\,S + E_{\text{free}} \leftrightharpoons I_{SE} \rightarrow P + E_{\text{free}}, \tag{B1}$$

where E_{free} is the unbound enzyme, I_{SE} is the substrate-enzyme intermediate, such that $E_{\text{free}} + I_{SE} = E$ with E denoting the total concentration of enzymes. In the remainder of this section, we focus on $n = 1$, which is sufficient to show that saturating kinetics only diminish any benefit coming from a condensed phase. This motivates our decision to use the limit of unsaturated enzymes beginning in Sec. B. With $n = 1$ the reaction (B1) is governed by the kinetic equations

$$\frac{dS}{dt} = -k_+S\,(E - I_{SE}) + k_-I_{SE}, \tag{B2a}$$

$$\frac{dI_{SE}}{dt} = k_+S\,(E - I_{SE}) - (k_- + k_{\text{cat}})I_{SE}, \tag{B2b}$$

$$\frac{dE_{\text{free}}}{dt} = -k_+S\,(E - I_{SE}) + (k_- + k_{\text{cat}})I_{SE}, \tag{B2c}$$

$$\frac{dP}{dt} = k_{\text{cat}}I_{SE}, \tag{B2d}$$

where k_+ is the rate of substrate binding to the enzyme, k_- is the rate of substrate unbinding from the enzyme before reacting, E is the total concentration of enzymes (free and bound), and $E_{\text{free}} = E - I_{SE}$ is the concentration of enzymes in the unbound state. In the steady-state approximation, $dI_{SE}/dt = 0$, which allows us to rearrange Eq. (B2b) to obtain

$$I_{SE} = \frac{k_+SE}{k_+S + k_- + k_{\text{cat}}}. \tag{B3}$$

Inserting this into Eq. (B2d), we recover the Michaelis-Menten result

$$\frac{dP}{dt} = k_{\text{cat}}E\,\frac{S}{\frac{k_{\text{cat}}+k_-}{k_+}+S} = v_{\max}\,\frac{S}{K_M+S}, \tag{B4}$$

where $v_{\max} = k_{\text{cat}}E$ and $K_M = (k_{\text{cat}} + k_-)/k_+$ is the Michaelis-Menten constant. We can gain some further physical intuition by rearranging this result as follows:

$$\frac{dP}{dt} = Ek_+S \cdot \frac{k_{\text{cat}}+k_-}{k_{\text{cat}}+k_-+k_+S} \cdot \frac{k_{\text{cat}}}{k_{\text{cat}}+k_-} = E \cdot k_+S \cdot P_{\text{free}} \cdot P_{\text{cat}}. \tag{B5}$$

This expression gives the turnover rate for each enzyme as the product of three terms. The first term k_+S describes the attempt rate for enzyme-substrate binding. These attempts are successful if the enzyme is not already in the bound state, which is given by $P_{\text{free}} = (k_{\text{cat}} + k_-)/(k_{\text{cat}} + k_- + k_+S)$. The last factor describes the success of bound enzyme-substrate complexes, of which only a fraction $P_{\text{cat}} = k_{\text{cat}}/(k_{\text{cat}} + k_-)$ proceed to catalysis without unbinding first.

2. Condensate Michaelis-Menten

Next we generalize the Michaelis-Menten scheme to account for reactions occurring within a condensate. The reaction scheme takes the form

$$S + B \leftrightharpoons I_{SB}, \tag{B6a}$$

$$I_{SB} + E \leftrightharpoons I_{SBE} \rightarrow P + E + B. \tag{B6b}$$

The two intermediates are the substrate bound to the scaffold I_{SB} and the substrate-scaffold-enzyme ternary complex I_{SBE}. This scheme allows for two steps that can saturate, condensate recruitment and catalysis, each of which will have a Michaelis-Menton constant. The Michaelis-Menton constant $K_{M,i}$ appearing in the manuscript will be determined by the step that is limiting at a lower concentration. Note that this scheme neglects direct enzyme-substrate binding, which provides another pathway for substrate turnover. However, if the condensate provides a kinetic benefit, the pathway in Eqs. (B6b) will dominate. This allows us to gain intuition despite neglecting the solution pathway. We will return to this approximation later.

The rate equations for this scheme are

$$\frac{dS_{\text{Is}}}{dt} = -k_{\text{on}}S_{\text{Is}}\,(B - I_{SB} - I_{SBE}) + k_{\text{off}}I_{SB}, \tag{B7a}$$

$$\frac{dI_{SB}}{dt} = k_{\text{on}}S_{\text{Is}}\,(B - I_{SB} - I_{SBE}) - k_{\text{off}}I_{SB} - k_+I_{SB}\,(E - I_{SBE}) + k_-I_{SBE}, \tag{B7b}$$

$$\frac{dI_{SBE}}{dt} = k_+I_{SB}\,(E - I_{SBE}) - (k_- + k_{\text{cat}})I_{SBE}, \tag{B7c}$$

$$\frac{dP}{dt} = k_{\text{cat}}I_{SBE}, \tag{B7d}$$

where k_+ is the rate that scaffold-bound substrates bind to the enzyme, k_- is the rate the I_{SBE} ternary complex breaks into a scaffold-bound substrate and an enzyme prior to reacting, B is the concentration of nonenzyme substrate binding sites on the condensate scaffold, the quantity $(B - I_{SB} - I_{SBE})$ is the

concentration of free substrate-binding sites on the scaffold, and $(E - I_{SBE})$ is the concentration of unbound enzyme. In the steady-state approximation we have $dI_{SB}/dt = dI_{SBE}/dt = 0$. From Eq. (B7c), we have

$$I_{SBE} = E\frac{I_{SB}k_+}{k_+I_{SB} + k_- + k_{\rm cat}} = E\,\frac{I_{SB}}{I_{SB} + K_{\rm Mrxn}}, \tag{B8}$$

where $K_{\rm Mrxn} = (k_- + k_{\rm cat})/k_+$ is a Michaelis-Menten parameter describing the reaction catalysis step within a condensate. Inserting Eq. (B8) into Eq. (B7d), we obtain a useful relationship

$$\frac{dP}{dt} = k_{\rm cat}E\,\frac{I_{SB}}{I_{SB} + K_{\rm Mrxn}}. \tag{B9}$$

The advantage of condensates in facilitating reactions is the increased concentrations they enable. In Eq. (B9), I_{SB} is the enhanced substrate concentration that is enabled by the condensate. However, Eq. (B9) shows there are diminishing returns to the increased concentration because if $I_{SB} > K_{\rm Mrxn}$ the reaction rate saturates at $v_{\rm max} = Ek_{\rm cat}$. Therefore, for the condensate to be beneficial, it is necessary that $K_{\rm Mrxn} > I_{SB}$. This conclusion can also be obtained from the small σ limit of Figs. 2(a) and 2(b), which corresponds to the unsaturated limit. Furthermore, reduced mobility within the condensate will reduce k_+ relative to the dilute phase, which will increase $K_{\rm Mrxn}$. This reduces the reaction rate for a given substrate concentration, but allows for higher substrate concentrations before the enzymes saturate.

To make further progress, we use the steady-state condition $dI_{SB}/dt = 0$ in combination with Eq. (B7b) to obtain

$$0 = k_{\rm on}S_{\rm Is}(B_i - I_{SB} - I_{SBE}) - I_{SB}(k_{\rm off} + k_+(E - I_{SBE})) + k_-I_{SBE}, \tag{B10}$$

which can be used with Eq. (B8) to obtain a quadratic equation for I_{SB}

$$0 = BK_{\rm Mrxn} - I_{SB}(\psi K_{\rm Mrxn} + E\eta - B) + I_{SB}^2\left(\frac{k_+}{k_{\rm on}S_{\rm Is}}E - \psi\right), \tag{B11}$$

where

$$\psi = 1 + \frac{k_{\rm off}}{k_{\rm on}S_{\rm Is}} + \frac{k_+}{k_{\rm on}S_{\rm Is}}E, \tag{B12}$$

$$\eta = 1 - \frac{k_-}{k_{\rm on}S_{\rm Is}}. \tag{B13}$$

The solution is

$$I_{SB} = \frac{-1}{2\left(1 + \frac{k_{\rm off}}{k_{\rm on}S_{is}}\right)}\left[(\psi K_{\rm Mrxn} + E\eta - B) - \sqrt{(\psi K_{\rm Mrxn} + E\eta - B)^2 + 4BK_{\rm Mrxn}\left(1 + \frac{k_{\rm off}}{k_{\rm on}S_{\rm Is}}\right)}\right], \tag{B14}$$

where we have chosen the solution that gives the limit $I_{SB} \simeq B$ when $S_{\rm Is} \to \infty$. As discussed above, the interesting regime is large $K_{\rm Mrxn}$ because condensates are not helpful unless $I_{SB} < K_{\rm Mrxn}$ [Eq. (B9)]. That means we are interested in the regime where $B/K_{\rm Mrxn} \ll 1$, which allows us to Taylor expand the square root

$$I_{SB} \simeq \frac{B}{\left(1 + \frac{k_{\rm off}}{k_{\rm on}S_{\rm Is}} + \frac{k_+}{k_{\rm on}S_{\rm Is}}E + \frac{E-B}{K_{\rm Mrxn}} - E\frac{k_-}{k_{\rm on}S_{\rm Is}K_{\rm Mrxn}}\right)}, \tag{B15}$$

$$I_{SB} \simeq \frac{B}{\left(1 + \frac{K_{\rm Mcond}}{S_{\rm Is}}\right)}, \tag{B16}$$

where the last step comes from neglecting terms of order $K_{\rm Mrxn}^{-1}$ and $K_{\rm Mcond} = (k_{\rm off} + k_+E)/k_{\rm on}$ is the Michaelis-Menten constant that describes the saturation of condensate binding sites. When available binding sites are not limiting $(S_{\rm Is} < K_{\rm Mcond})$, the intermediate concentration is approximately $I_{SB} \simeq BS_{\rm Is}/K_{\rm Mcond}$, which can be combined with Eq. (B9) to give an equation in the form of Eq. (1) with $K_{M,\rm I}^1 = K_{\rm Mcond}K_{\rm Mrxn}/B$ and $k_{\rm I} = k_{\rm cat}$. However, this equation describes the case of saturating enzyme kinetics where the condensate is not beneficial. A more interesting limit is in the unsaturated regime where $K_{\rm Mrxn} \gg I_{SB}$.

The reaction rate in the limit of unsaturated enzymes is obtained by inserting Eq. (B16) into Eq. (B7d)

$$\frac{dP}{dt} = k_{\rm cat}E\,\frac{I_{SB}}{I_{SB} + K_{\rm Mrxn}} \tag{B17}$$

$$\simeq k_{\rm cat}E\,\frac{1}{K_{\rm Mrxn}}\,\frac{B}{\left(1 + \frac{K_{\rm Mcond}}{S_{\rm Is}}\right)}, \tag{B18}$$

where again, we have used $K_{\rm Mrxn} \gg I_{SB}$. Inserting the definitions of $K_{\rm Mrxn}$, $K_{\rm Mcond}$, and rearranging, we find

$$\begin{aligned}\frac{dP}{dt} &\simeq k_{\rm cat}E \cdot \frac{B}{K_{\rm Mrxn}} \cdot \frac{S_{\rm Is}}{(S_{\rm Is} + K_{\rm Mcond})} \\ &\simeq BS_{\rm Is}k_{\rm on} \cdot \frac{k_{\rm cat}}{k_- + k_{\rm cat}} \cdot \frac{k_+E}{k_{\rm off} + k_+E} \cdot \frac{k_{\rm off} + k_+E}{(S_{\rm Is}k_{\rm on} + k_{\rm off} + k_+E)} \\ &\simeq B(S_{\rm Is}k_{\rm on}) \cdot P_{\rm cat} \cdot P_{\rm enz} \cdot P_{\rm free}.\end{aligned}$$

Just as we found that the solution Michaelis-Menten case can be written as a product of probabilities (Eq. (B5)), we see that the condensate-mediated reaction rate can be written as the product of a binding attempt rate $(S_{\rm Is}k_{\rm on})$, the probability that the binding site is free $P_{\rm free}$, the probability the substrate transfers to the enzyme before unbinding $P_{\rm enz}$, and the probability that catalysis occurs before detaching from the enzyme $P_{\rm cat}$. This product does not capture events where the substrate binds to the enzyme multiple times before catalysis $I_{SB} \leftrightharpoons I_{SBE}$. The terms describing these events were lost in the Taylor expansion and subsequent neglect of terms of order $K_{\rm Mrxn}^{-1}$.

APPENDIX C: REACTION RATE ENHANCEMENT BY CONDENSATES

In this Appendix, we provide the mathematical details for the calculation of the reaction rate enhancement, defined as $\mathcal{E} = \bar{R}/R_{\rm homo}$. Here we assume that clients maintain mobility and we do not distinguish between bound and unbound

fractions [see Eq. (A16) and related discussion to justify this simplification]. From the conservation of mass condition, it follows:

$$\bar{S} = S_{\rm I}\,\phi + S_{\rm II}(1-\phi) = S_{\rm II}\left(1-\phi+\frac{S_{\rm I}}{S_{\rm II}}\,\phi\right) = S_{\rm II}(1-\phi+p_S\,\phi), \tag{C1}$$

i.e.,

$$S_{\rm II} = \frac{\bar{S}}{1-\phi+p_S\,\phi}, \quad S_{\rm I} = \frac{p_S\,\bar{S}}{1-\phi+p_S\,\phi}, \quad p_S = \frac{S_{\rm I}}{S_{\rm II}}. \tag{C2}$$

Similarly, we obtain for the enzyme E:

$$E_{\rm II} = \frac{\bar{E}}{1-\phi+p_E\,\phi}, \quad E_{\rm I} = \frac{p_E\,\bar{E}}{1-\phi+p_E\,\phi}, \quad p_E = \frac{E_{\rm I}}{E_{\rm II}}. \tag{C3}$$

The reaction rate in the homogeneous system is given by the Michaelis-Menten-Hill equation

$$R_{\rm homo} = \frac{k_{\rm II}\,\bar{E}\,\bar{S}^n}{K_M^n+\bar{S}^n}, \tag{C4}$$

where n is the Hill coefficient, K_M is the unscaffolded Michaelis-Menten constant, and we have assumed that the rate constant in the homogeneous state equals that of the dilute phase, i.e., $k_{\rm II}$. The reaction rate inside the condensate is

$$R_{\rm I} = \frac{k_{\rm I}\,E_{\rm I}\,S_{\rm I}^n}{K_{M,{\rm I}}^n+S_{\rm I}^n} = k_{\rm I}\,\frac{p_E\,\bar{E}}{(1-\phi+p_E\,\phi)}\,\frac{p_S^n\,\bar{S}^n}{\left[K_{M,{\rm I}}^n(1-\phi+p_S\,\phi)^n+p_S^n\,\bar{S}^n\right]}, \tag{C5}$$

where $K_{\rm Mrxn}$ is the scaffolded Michaelis-Menten constant. The rate outside the condensate is

$$R_{\rm II} = \frac{k_{\rm II}\,E_{\rm II}\,S_{\rm II}^n}{K_{M,{\rm II}}^n+S_{\rm II}^n} = k_{\rm II}\,\frac{\bar{E}}{(1-\phi+p_E\,\phi)}\,\frac{\bar{S}^n}{\left[K_{M,{\rm II}}^n(1-\phi+p_S\,\phi)^n+\bar{S}^n\right]}. \tag{C6}$$

The volume averaged reaction rate is then

$$\bar{R} = R_{\rm I}\,\phi + R_{\rm II}(1-\phi) = k_{\rm II}\,\frac{\bar{E}\,\bar{S}^n}{(1-\phi+p_E\,\phi)}\left(\frac{k_{\rm I}}{k_{\rm II}}\,\frac{\phi\,p_E\,p_S^n}{K_{M,{\rm I}}^n(1-\phi+p_S\,\phi)^n+p_S^n\,\bar{S}^n}+\frac{1-\phi}{K_{M,{\rm II}}^n(1-\phi+p_S\,\phi)^n+\bar{S}^n}\right). \tag{C7}$$

Assuming equal partitioning for substrate and enzyme, i.e., $p_S = p_E = p$, we find

$$\mathcal{E} = \frac{\bar{R}}{R_{\rm homo}} = \frac{\mu^n(1+\sigma^n)}{(1-\phi+p\,\phi)}\left(\kappa\,\frac{\phi\,p}{\left(\frac{1-\phi}{p}+\phi\right)^n+\sigma^n\mu^n}+\frac{1-\phi}{\omega^n\,(1-\phi+p\phi)^n+\sigma^n\mu^n}\right), \tag{C8}$$

where

$$\sigma = \frac{\bar{S}}{K_M}, \quad \kappa = \frac{k_{\rm I}}{k_{\rm II}}, \quad \mu = \frac{K_M}{K_{M,{\rm I}}}, \quad \omega = \frac{K_{M,{\rm II}}}{K_{M,{\rm I}}}. \tag{C9}$$

The reaction rate enhancement $\mathcal{E}$ is a function of 6 dimensionless parameters: ϕ, p, σ, κ, μ and ω. We now study the behavior of this function in dependence of these parameters (see Fig. 2 of the main text for details).

(i) Dependence on $\boldsymbol{\kappa}$. The rate enhancement function increases linearly with κ. The dependence of $\mathcal{E}$ on κ is therefore straight forward.

(ii) Dependence on $\boldsymbol{\mu}$. The rate enhancement function increases monotonically with μ. The dependence of $\mathcal{E}$ on μ is of the form $\mu^n/(1+\alpha\mu^n)$, which is always an increasing function of μ.

(iii) Dependence on $\boldsymbol{\omega}$. $\mathcal{E}$ decreases with increasing ω.

Therefore the dependence of $\mathcal{E}$ on the parameters κ, μ and ω is trivial. The dependence of $\mathcal{E}$ on σ exhibits more interesting behavior.

(i) Dependence on $\boldsymbol{\sigma}$. When the substrate concentration is very large, $\sigma\to\infty$, the condensate provides little or no enhancement. The rate enhancement in this case becomes

$$\lim_{\sigma\to\infty}\mathcal{E} = \frac{1-\phi+\kappa\,p_E\,\phi}{1-\phi+p_E\,\phi} = 1+\frac{(\kappa-1)\,p_E\,\phi}{1-\phi+p_E\,\phi}. \tag{C10}$$

From this formula, we see that if $\kappa\leqslant 1$, then $\lim_{\sigma\to\infty}\rho\leqslant 1$, with equality when $\kappa=1$. Significant rate enhancement is obtained in the opposite limit of low substrate concentration $\sigma\to 0$. In this limit

$$\lim_{\sigma\to 0}\mathcal{E} = \left(\frac{\mu}{\omega}\right)^n\frac{1-\phi+\omega^n\kappa\,\phi\,p^{n+1}}{(1-\phi+p\,\phi)^{n+1}}. \tag{C11}$$

This is Eq. (3) from the main text.

(ii) Dependence on $\boldsymbol{\phi}$. As discussed above, condensates are beneficial for the reaction rate at low substrate concentration. Therefore we focus on the behavior of the enhancement function $\mathcal{E}$ in the limit $\sigma\to 0$, Eq. (C11). This function displays a maximum as a function of condensate volume fraction ϕ. We find the maximum of $\mathcal{E}$ by setting $\partial\mathcal{E}/\partial\phi = 0$ using Eq. (C11), which yields

$$\phi^\star = \frac{(\omega^n\kappa\,p^{n+1}-1)-(n+1)(p-1)}{n(p-1)(\omega^n\kappa\,p^{n+1}-1)}. \tag{C12}$$

APPENDIX D: MOBILITY LOSS UPON BINDING IMPAIRS REACTION RATES

Consider the situation where the species bound to the condensate are immobile. This means that reactions are limited to collisions with soluble species. This is known as the Eley-Rideal mechanism [33]. This mechanism describes situations where the enzymes are covalently bound to the scaffolds [14,15] or the clients are recruited by specific binding modules [22].

1. Instantaneous reaction rates

In the unsaturated limit, the reaction rate in the dilute phase is $R_{\rm II} = k'_{\rm II} S^n_{\rm II} E_{\rm II}$, where $k'_{\rm II} = k_{\rm cat}/K^n_{M,{\rm II}}$ is the linearized rate constant. Inside the condensate we impose the requirement that, at most, only one species can be bound for the reaction to proceed. To enforce this requirement we separate the enzyme and substrate concentrations into bound and soluble fractions. This gives the reaction rate

$$R_{\rm I} = k'_{\rm I}\left(S^n_{\rm Is} E_{\rm Is} + S^n_{\rm Is} E_{\rm Ib} + S_{\rm Ib} S^{n-1}_{\rm Is} E_{\rm Is}\right), \tag{D1}$$

where $k'_{\rm I}$ is the linearized rate constant in the dense phase. The volume averaged rate is $\bar{R} = (1-\phi)R_{\rm II} + \phi R_{\rm I}$, where $\phi = V_{\rm I}/V_{\rm tot}$ is the volume fraction of the dense phase. If the reaction rate constants are equal in the two phases, $k'_{\rm I} = k'_{\rm II} = k$, and the system is in diffusive equilibrium across the condensate interface so that $S_{\rm II} = S_{\rm Is}$ and $E_{\rm II} = E_{\rm Is}$ (both approximations are strongly favorable for condensate reactions), then the average reaction rate in the two-phase system is

$$\bar{R} = k S^{n-1}_{\rm II}[S_{\rm II} E_{\rm II} + \phi(S_{\rm II} E_{\rm Ib} + S_{\rm Ib} E_{\rm II})]. \tag{D2}$$

This should be compared to the system with homogeneous concentrations $\bar{S} = (1-\phi)S_{\rm II} + \phi S_{\rm I} = S_{\rm II} + \phi S_{\rm Ib}$, $\bar{E} = (1-\phi)E_{\rm II} + \phi E_{\rm I} = E_{\rm II} + \phi E_{\rm Ib}$ and total rate

$$R_{\rm hom} = k\bar{S}^n \bar{E} \tag{D3}$$

$$= k\bar{S}^{n-1}[S_{\rm II} E_{\rm II} + \phi(S_{\rm II} E_{\rm Ib} + S_{\rm Ib} E_{\rm II}) + \phi^2 S_{\rm Ib} E_{\rm Ib}]. \tag{D4}$$

The rate $R_{\rm hom}$ is clearly greater than the total rate $\bar{R}$ in the phase-separated system since $\bar{S} > S_{\rm II}$ and $\bar{R}$ lacks the ϕ^2 term. The missing term is due to the fact that molecule pairs that were immobilized in the phase-separated system are able to react in the homogeneous system. The most favorable case is $n = 1$ and $S_{\rm Ib} = 0$, which describes a condensed enzyme and a substrate that does not bind the scaffold [14,15]. In this case, $\bar{R} = R_{\rm hom}$, so the reaction rate is identical to that of a well-mixed system in the absence of condensate. Therefore, in the Eley-Rideal limit, condensates are either neutral or detrimental to reaction kinetics.

2. Numerical solution of rate equations when bound reactants are immobile

Depletion of substrate within the condensate further inhibits reactions. The above analysis only considers the instantaneous rate at the beginning of the reaction. After the reaction begins there will be additional limitations due to diffusive transport between $V_{\rm I}$ and $V_{\rm II}$ and the exchange between bound and unbound states in the condensate. To understand these kinetic factors we consider the case where the enzyme is covalently linked to the scaffold, so $E_{\rm Is} = 0$, and allow the S concentrations to vary with time. The kinetic equations for $n = 1$ are

$$\frac{dS_{\rm Is}}{dt} = k_{\rm diff}(S_{\rm II} - S_{\rm Is}) - k_{\rm on}[S_{\rm Is}(B - S_{\rm Ib}) - K_D S_{\rm Ib}] - k S_{\rm Is} E_{\rm I}, \tag{D5a}$$

$$\frac{dS_{\rm Ib}}{dt} = k_{\rm on}[S_{\rm Is}(B - S_{\rm Ib}) - K_D S_{\rm Ib}], \tag{D5b}$$

$$\frac{dS_{\rm II}}{dt} = -\frac{\phi}{1-\phi} k_{\rm diff}(S_{\rm II} - S_{\rm Is}) - k S_{\rm II} E_{\rm II}. \tag{D5c}$$

The concentration of soluble S particles within the condensate can change via three processes. The first term $k_{\rm diff}(S_{\rm II} - S_{\rm Is})$ describes the diffusive flux between the dense and dilute phases. The exchange between the inner and outer volumes is modeled by the Smoluchowski flux $4\pi D R_{\rm cond}(S_{\rm II} - S_{\rm Is})$ divided by the volume of the condensate $4\pi R^3_{\rm cond}/3$. Therefore $k_{\rm diff} = 3D/R^2_{\rm cond}$, where D is the diffusion constant of the S species and $R_{\rm cond}$ is the condensate radius. The second term $k_{\rm on}[S_{\rm Is}(B - S_{\rm Ib}) - K_D S_{\rm Ib}]$ describes the binding and unbinding of S molecules to binding sites on the scaffolds in the condensate. We assume the scaffold matrix provides binding sites at a concentration B of which $B - S_{\rm Ib}$ are available to bind S at a rate constant $k_{\rm on}$. The rate at which S are released from the scaffold, $k_{\rm off}$, is expressed in terms of the dissociation constant $K_D = k_{\rm off}/k_{\rm on}$. The third term in Eq. (D5a) describes S particles reacting with E, where again we have made the optimistic approximation that the rate constants in the dilute and dense phases are identical $k'_{\rm I} = k'_{\rm II} = k$. Equation (D5b) describes the concentration of S particles that are bound to the condensate. Equation (D5c) describes the concentration of S particles outside of the condensate, which can change by either diffusive exchange with the condensate or reactions with E with rate $R_{\rm II}$. The diffusion term in Eq. (D5c) depends on ϕ reflecting the unequal volumes of the phases.

Figure 6 plots the condensate enhancement factor, which we define as the time required for the reaction to consume half of the S particles in the homogeneous system divided by the separated system. The former quantity is computed from $k^{-1}\bar{E}^{-1}\ln 2$, while the latter quantity is determined by numerical solution of Eqs. (D5a)–(D4c). In all cases the enhancement factor is less than one, indicating that the presence of the condensate has an *inhibitory* effect on the reaction rate. This is true whether the system is initialized from a homogeneous state, $S_{\rm II} = S_{\rm Is} = \bar{S}$ and $S_{\rm Ib} = 0$ (Fig. 6), or if the system is started from a state where the S particles have reached an equilibrium binding to the condensate before reaction is started (data not shown).

Fast reactions. When the reaction rate is faster than the binding or diffusion timescales (Fig. 6, left panel) the condensed system most closely approaches the rate of the homogeneous system when $k_{\rm diff}$ is large and $k_{\rm on}$ is small. Large $k_{\rm diff}$ minimizes the inhibitory effect of transporting substrate to the enzymes in the condensate, while small $k_{\rm on}$ allows the substrate to react with immobile enzymes before it binds to the condensate.

Fast binding. When binding to the network is very fast (Fig. 6, center panel), the way to keep substrate in the unbound, reactive state is to keep the soluble substrate

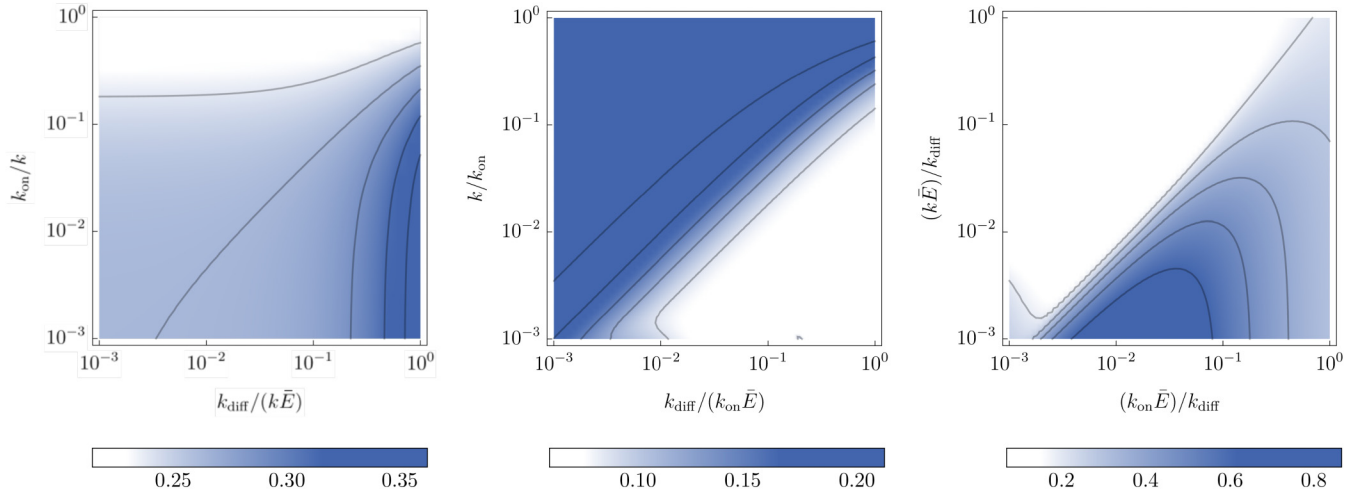

FIG. 6. Plot of the condensate enhancement factor as a function of the rate constants in Eq. (4). The enhancement factor compares the time to consume half of the reactant in the homogenous system to the separated system. Ratios less than one, which is the case in all conditions in the figure, indicate that it takes longer for the reaction to proceed in the separated system. In each panel, the fastest rate constant is held fixed (k in the left panel, k_{on} in the middle panel, and k_{diff} in the right panel) and the other two are varied over three orders of magnitude. See text for a brief description of each panel. Parameters as in Eq. (D5): $\phi = 0.1$, $B_I/\bar{E} = 8$, $\bar{B}/\bar{E} = 1$, $k_{diff} = 0.1$, and $\bar{S}_{t=0} = 2$. Here, $\bar{B} = \phi B_I + (1-\phi) B_{II}$ denotes the average B concentration.

concentration low (below K_D). This occurs when $k \gg k_{diff}$ so that the reaction consumes substrate as soon as it enters the condensate.

Fast diffusion. When the diffusion rate is much faster than the reaction or binding rates (Fig. 6, right panel), the inhibitory effect of substrate transport is negligible and the system approaches the reaction rate of the homogeneous system, provided the reaction consumes the incoming substrate faster than it can bind. If the reaction rate is too fast, however, diffusion can become limiting again. The optimal reaction rate in the right panel of Fig. 6, where the reaction proceeds at ∼80% of the rate of the homogeneous system, occurs when k is large enough to out-compete binding, but not so large that diffusion becomes limiting.

APPENDIX E: OPTIMAL PARTITIONING AFFINITY

Increasing the affinity of a client to the condensate comes at the cost of mobility. Here we determine the optimal affinity that balances the increase in concentration with the loss in mobility.

Increasing the affinity of clients to the network has three effects on the reaction rate enhancement $\mathcal{E}$. First, it reduces the dilute phase concentration, which reduces the reaction rate. Second, it increases the dense phase concentration, which increases the rate. Third, it decreases the mobility of reactants in the dense phase, which reduces the reaction rate. The first two effects are captured by the p dependencies in Eq. (C11), but the calculation in the main text shows that the optimal sticker affinity is given by $\ln(1 + e^{-\Delta f/k_B T}) = 2$, so $p = e^{2M}$ in the best case scenario.

The mobility effect is captured in the $\omega^n \kappa = k_I'/k_{II}'$ factor in Eq. (C11), where k_I' and k_{II}' are the linearized rate constants. In the subsaturated regime, these constants include the effects of both catalytic turnover and diffusion. Therefore we assume that the reaction rate inside the condensate k_I is proportional to the diffusion constant of the clients. The diffusion constant is proportional to $M^{-2}(1 + e^{-\Delta f/k_B T})^{-1}$ [Eq. (8) of main text, Eq. (A18)], but the term in parentheses is just another factor of e^2 that can be absorbed into the constant of proportionality. Therefore we write

$$\frac{k_I}{k_{II}} = \frac{\alpha}{M^2}, \tag{E1}$$

where α is a constant of proportionality (that will have minimal effect on the results).

Now we insert Eq. (E1) and partition coefficient $p = e^{2M}$ into Eq. (C11) and obtain

$$\mathcal{E} = \frac{(\mu^n/\omega^n)}{(1-\phi+\phi\, e^{2M})^{n+1}}\left(1 - \phi + \frac{\alpha}{M^2}\, e^{2M(n+1)}\phi\right). \tag{E2}$$

This expression has a (nonphysical) divergence at $M = 0$ and monotonically decreases at large M. There are two possible behaviors in-between, it can monotonically decrease, or there can be a local minima followed by a local maximum (Fig. 7).

To determine if there is an enhancement due to recruitment, we set $\frac{\partial \mathcal{E}}{\partial M} = 0$ and find that the reaction rate is greatest when the number of stickers is equal to the largest root of

$$M^2 = \alpha\, e^{2Mn}\left[1 - \frac{1}{M(n+1)}\left(1 + \frac{\phi}{1-\phi}e^{2M}\right)\right]. \tag{E3}$$

This is a transcendental equation that can be solved numerically to yield the optimal sticker number $M^\star$ [Fig. 7(d)]. If n is small or ϕ is large there are no solutions to Eq. (E3) indicating that recruitment to the condensate is detrimental to the reaction rate. However, large n and small ϕ favour highly partitioned systems as discussed in the text.

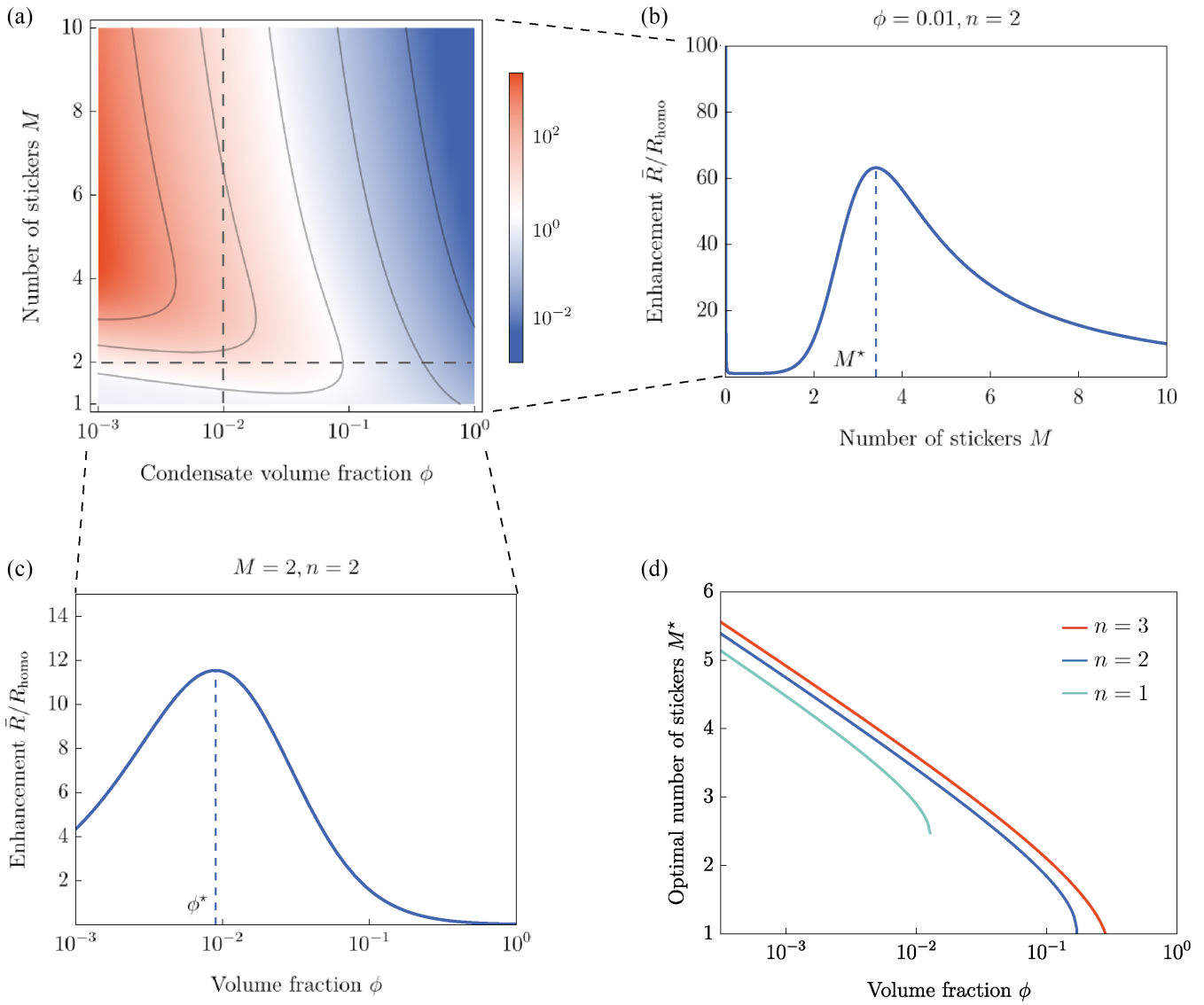

FIG. 7. (a) The reaction rate can have a pair of local extremes in terms of sticker number M (b) and volume fraction ϕ (c). (d) Small volume fractions and/or large reaction orders promote the appearance of the local maximum. Parameters: $\alpha = 0.05$.

Analysis of the asymptotics of Eq. (E3) reveals physical insights. We are looking for intersections between the left side and the right side. The physically relevant region is $M > 1$ but mathematical intuition can be gained by starting at $M = 0$.

(i) The left side starts at 0 at $M = 0$ and diverges to $+\infty$ as $M \to +\infty$.

(ii) The right side tends to $-\infty$ at $M = 0$ (dominated by the $1/M$ term) and also tends to $-\infty$ as $M \to +\infty$ (dominated by the e^{2M} term).

(iii) The right side can only intersect the left side if the term in square brackets is positive. Despite the fact that the left side increases rapidly with M, the right side diverges even faster due to the e^{2Mn} prefactor. Therefore even a slightly positive value in the square bracket is likely to give a root.

(iv) The biggest unknown in this equation is the constant α. While this parameter has a strong effect on the maximum rate within the dense phase, it has a very weak effect on the presence or location of the maximum. That is because the right side of the equation will be nearly vertical at the two roots, meaning that even an order of magnitude change in α will only change the location of the roots by $M \pm 1$.

(v) The interesting root, representing the rate maximum, is close to the largest value of M for which the term in the round parentheses is less than 1 (including the prefactor)

$$\frac{1}{M(n+1)}\left(1 + \frac{\phi}{1-\phi}e^{2M}\right) = 1. \tag{E4}$$

We see that the left hand side of Eq. (E4) increases very rapidly with M. Therefore no root of Eq. (E4) exists for $M \geqslant 2$ unless ϕ is sufficiently small and/or n is large. This explains why there is no solution for $M^\star$ when ϕ is above a certain threshold (see Fig. 7).

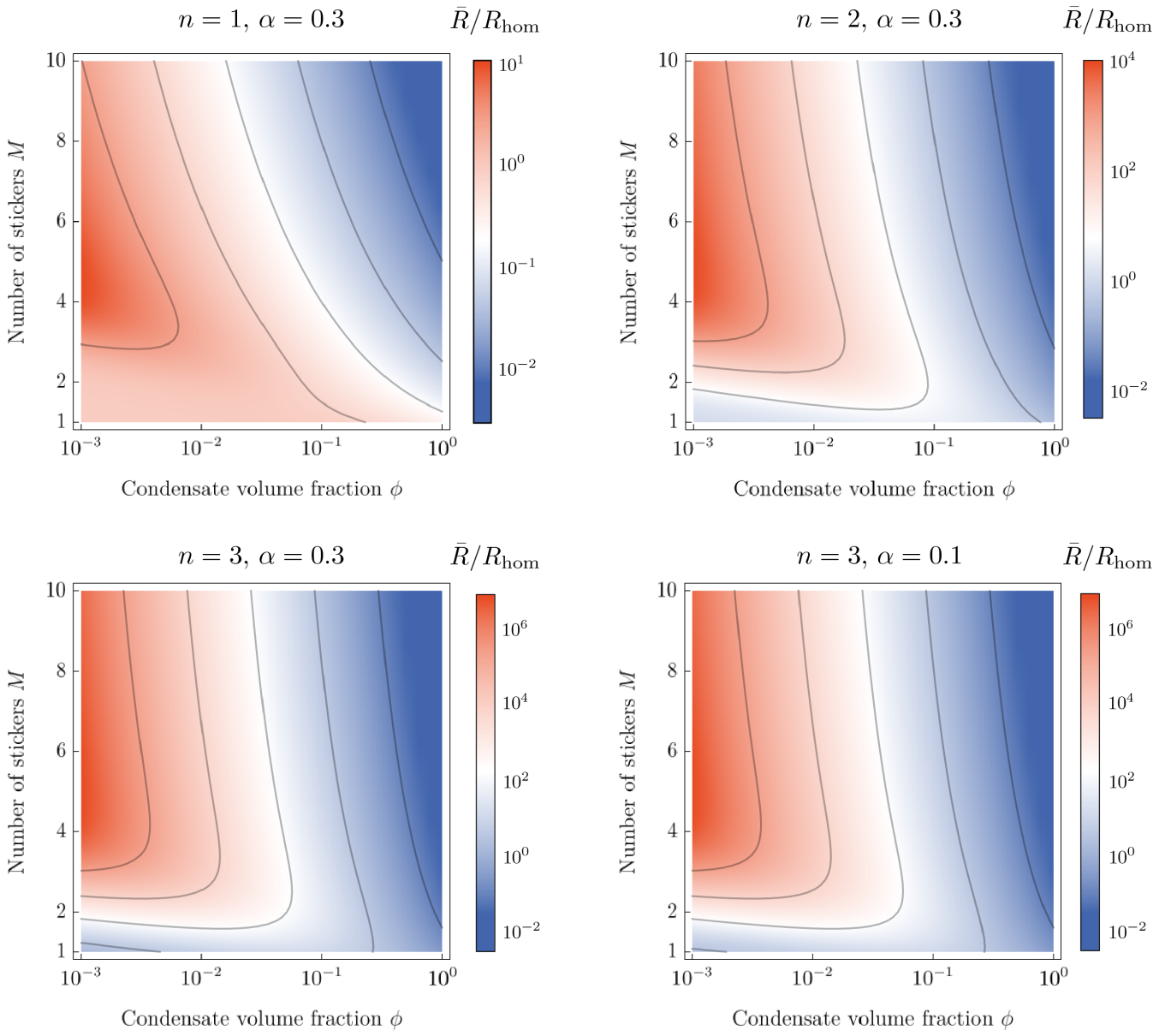

FIG. 8. Reaction rate enhancement as a function of the volume fraction ϕ and the number of stickers M. Varying the reaction n order makes a big difference to the reaction rate; however, changing α, the constant of proportionality between Stokes and reptation diffusion, has a limited effect on reaction rate.

[1] Y. Shin and C. P. Brangwynne, Science **357**, eaaf4382 (2017).

[2] S. F. Banani, H. O. Lee, A. A. Hyman, and M. K. Rosen, Nat. Rev. Mol. Cell Biol. **18**, 285 (2017).

[3] A. S. Lyon, W. B. Peeples, and M. K. Rosen, Nat. Rev. Mol. Cell Biol. **22**, 215 (2021).

[4] M. Hondele, S. Heinrich, P. De Los Rios, and K. Weis, Emerging Top. Life Sci. **4**, 343 (2020).

[5] J. A. Ditlev, L. B. Case, and M. K. Rosen, J. Mol. Biol. **430**, 4666 (2018).

[6] J. A. Riback, L. Zhu, M. C. Ferrolino, M. Tolbert, D. M. Mitrea, D. W. Sanders, M.-T. Wei, R. W. Kriwacki, and C. P. Brangwynne, Nature (London) **581**, 209 (2020).

[7] J. A. Riback, C. D. Katanski, J. L. Kear-Scott, E. V. Pilipenko, A. E. Rojek, T. R. Sosnick, and D. A. Drummond, Cell **168**, 1028 (2017).

[8] T. M. Franzmann, M. Jahnel, A. Pozniakovsky, J. Mahamid, A. S. Holehouse, E. Nüske, D. Richter, W. Baumeister, S. W. Grill, R. V. Pappu *et al.*, Science **359**, eaao5654 (2018).

[9] L. B. Case, X. Zhang, J. A. Ditlev, and M. K. Rosen, Science **363**, 1093 (2019).

[10] D. Deviri and S. A. Safran, Proc. Natl. Acad. Sci. USA **118**, e2100099118 (2021).

[11] C. P. Brangwynne, P. Tompa, and R. V. Pappu, Nat. Phys. **11**, 899 (2015).

[12] R. R. Poudyal, R. M. Guth-Metzler, A. J. Veenis, E. A. Frankel, C. D. Keating, and P. C. Bevilacqua, Nat. Commun. **10**, 490 (2019).
[13] R. R. Poudyal, C. D. Keating, and P. C. Bevilacqua, ACS Chem. Biol. **14**, 1243 (2019).
[14] A. M. Küffner, M. Prodan, R. Zuccarini, U. Capasso Palmiero, L. Faltova, and P. Arosio, ChemSystemsChem **2**, syst.202000001 (2020).
[15] M. Guan, M. V. Garabedian, M. Leutenegger, B. S. Schuster, M. C. Good, and D. A. Hammer, Biochemistry **60**, 3137 (2021).
[16] K. Le Vay, E. Y. Song, B. Ghosh, T. Y. Tang, and H. Mutschler, Angew. Chem., Int. Ed. **60**, 26096 (2021).
[17] J. D. Schmit, E. Kamber, and J. Kondev, Phys. Rev. Lett. **102**, 218302 (2009).
[18] M. Feric and T. Misteli, BioEssays **44**, 2200001 (2022).
[19] J. Wang, J.-M. Choi, A. S. Holehouse, H. O. Lee, X. Zhang, M. Jahnel, S. Maharana, R. Lemaitre, A. Pozniakovsky, D. Drechsel *et al.*, Cell **174**, 688 (2018).
[20] E. W. Martin, A. S. Holehouse, I. Peran, M. Farag, J. J. Incicco, A. Bremer, C. R. Grace, A. Soranno, R. V. Pappu, and T. Mittag, Science **367**, 694 (2020).
[21] W. Peeples and M. K. Rosen, Nat. Chem. Biol. **17**, 693 (2021).
[22] S. F. Banani, A. M. Rice, W. B. Peeples, Y. Lin, S. Jain, R. Parker, and M. K. Rosen, Cell **166**, 651 (2016).
[23] M. Rubinstein, R. H. Colby *et al.*, *Polymer Physics* (Oxford University Press, New York, 2003), Vol. 23.
[24] M. Doi and S. F. Edwards, *The Theory of Polymer Dynamics* (Oxford University Press, Oxford, 1988), Vol. 73.
[25] K. Luby-Phelps, Mol. Biol. Cell **24**, 2593 (2013).
[26] D. W. Sanders, N. Kedersha, D. S. Lee, A. R. Strom, V. Drake, J. A. Riback, D. Bracha, J. M. Eeftens, A. Iwanicki, A. Wang *et al.*, Cell **181**, 306 (2020).
[27] S. S. Mogre, A. I. Brown, and E. F. Koslover, Phys. Biol. **17**, 061003 (2020).
[28] W. Pönisch, T. C. Michaels, and C. A. Weber, Biophys. J. **122**, 197 (2023).
[29] C. Weber, T. Michaels, and L. Mahadevan, eLife **8**, e42315 (2019).
[30] F. Geiger, J. Acker, G. Papa, X. Wang, W. E. Arter, K. L. Saar, N. A. Erkamp, R. Qi, J. P. Bravo, S. Strauss *et al.*, EMBO J. **40** e107711 (2021).
[31] I. Seim, C. A. Roden, and A. S. Gladfelter, Biophys. J. **120**, 2771 (2021).
[32] C. C. Correll, J. Bartek, and M. Dundr, Cells **8**, 869 (2019).
[33] W. H. Weinberg, Acc. Chem. Res. **29**, 479 (1996).